Effective Mass for Holes in Paramagnetic, Plasmonic Cu_5FeS_4 Semiconductor Nanocrystals

Jason E. Kuszynski,[a] Joshua C. Kays,[b] Carl R. Conti III,[a] Stephen A. McGill,[c] Allison M. Dennis[b,d] and Geoffrey F. Strouse*[a]

a. Department of Chemistry and Biochemistry, Florida State University, Tallahassee FL 32306, USA.

b. Department of Biomedical Engineering, Boston University, Boston MA 02215, USA.

c. National High Magnetic Field Laboratory, Tallahassee FL 32310, USA.

d. Division of Materials Science & Engineering, Boston University, Boston MA 02215, USA.

Contents

Figure S1. Transmission Electron Microscopy and Powder X-Ray Diffraction of Cu$_5$FeS$_4$.

Representative transmission electron microscopy (TEM) from Kays et al.[1] (**A**) and powder X-ray diffraction (pXRD) patterns (**B**) were collected using a Rigaku MiniFlex powder X-ray diffractometer equipped with a Cu-Kα source. Samples were dried, powdered, and loaded onto a Rigaku zero-background micropowder plate. Scans were acquired from 20-70° 2θ at a rate of 5°/min and a 0.1° step size. Whole powder pattern fitting and the Halder-Wagner method for Scherrer analysis were completed using the Rigaku SmartLab Studio software and performed for all NCs. The pXRD of Cu_5FeS_4 obtained indicates a good match with the high cubic bulk Bornite phase. (ICSD card number 24174)

Figure S2. MCD Instrument Calibration Using Gold Nanoparticles
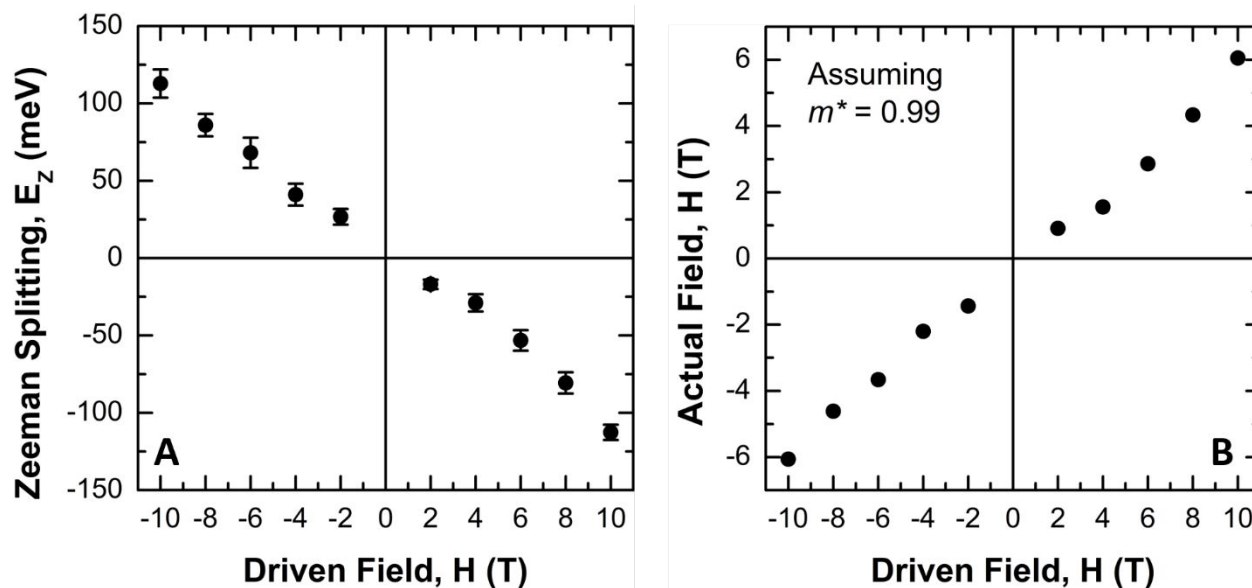
6.2 nm gold nanoparticles were utilized as an external reference to calibrate the sign of dichroism of the MCD instrument and ensure that m^* is correctly calculated across the 10 T driven field sweep. (**A**) MCD spectra were collected for gold nanoparticles in toluene solution located in the stray field of the Cryostat at 298 K at the driven fields referenced. (**B**) Subsequently, the Zeeman splitting energy was calculated from the Python fitting routine, where the actual field

experienced by the particles could be calculated utilizing 0.99 m^*/m_e as a reference,[2] showcasing

expected linear Zeeman splitting behavior from the applied stray field.

Figure S3. Full VH-MCD spectra of Cu_5FeS_4 PSNCs.

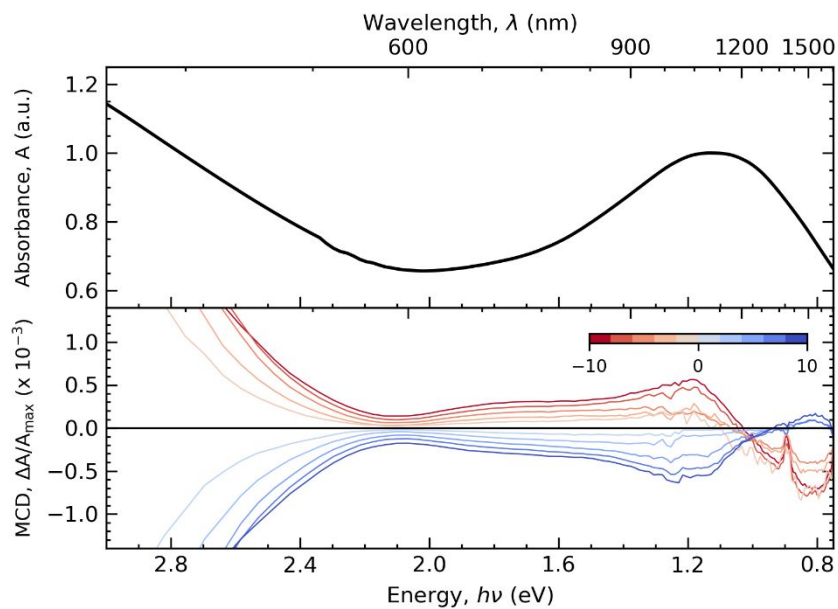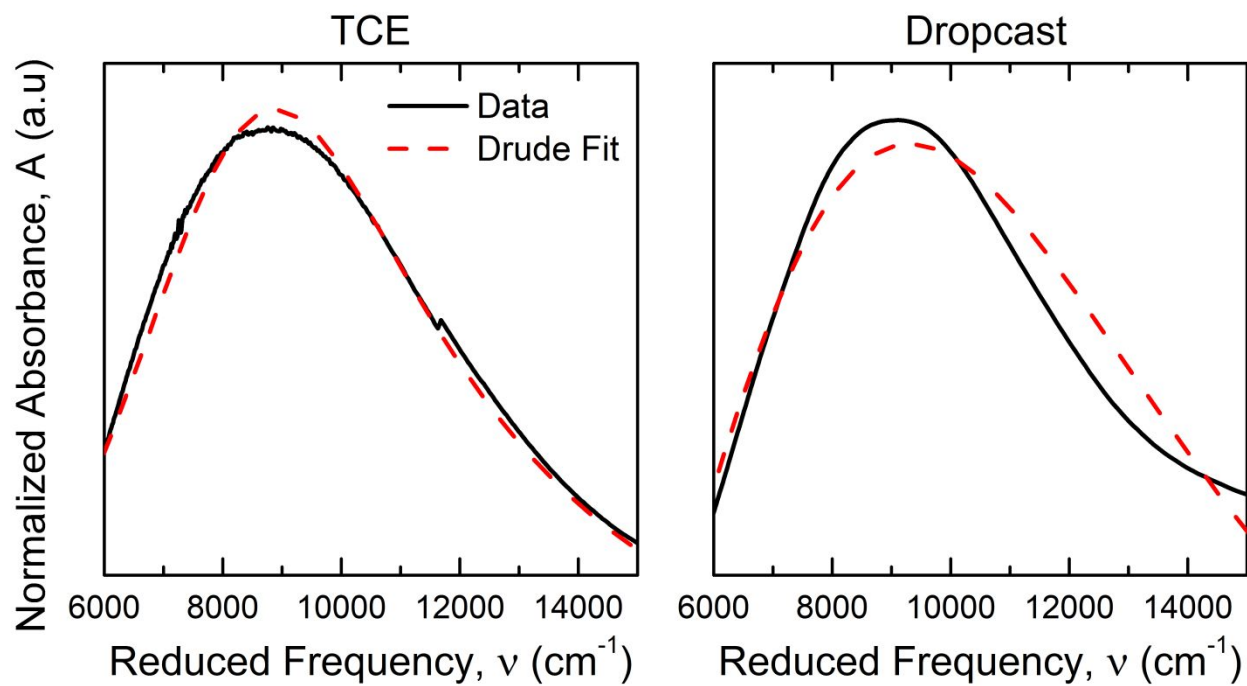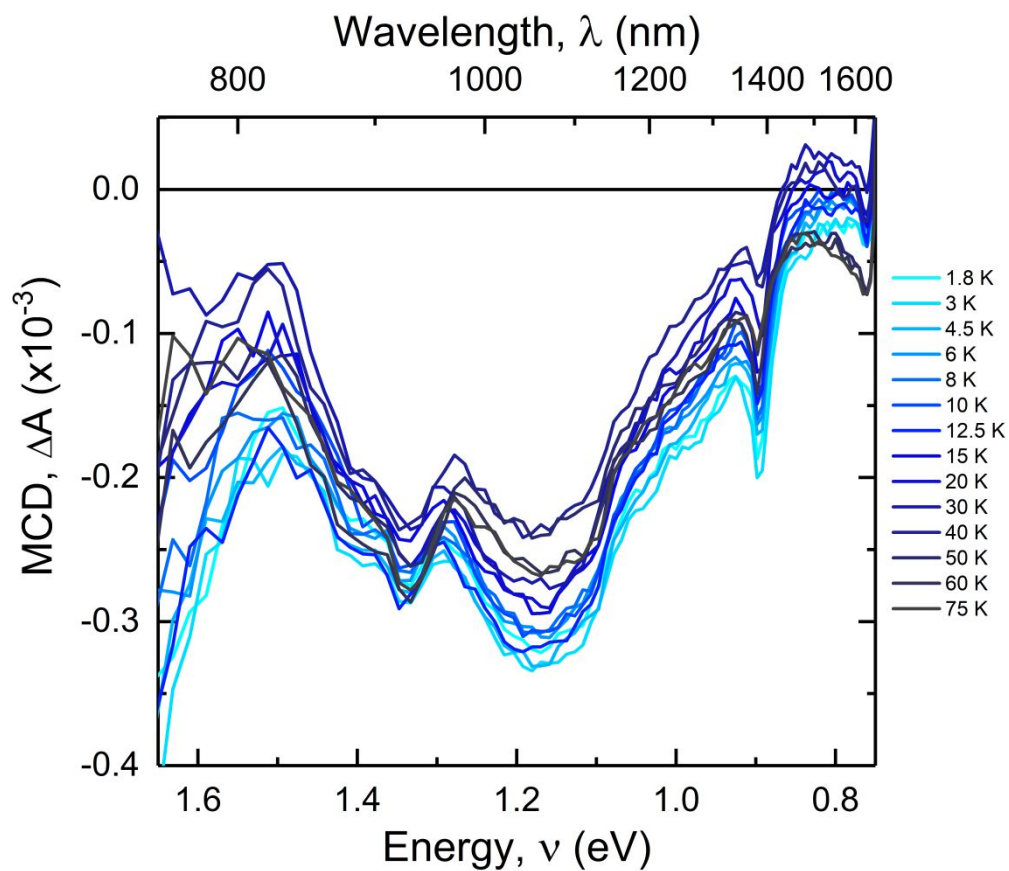**Figure S4. Frequency-independent Drude modelling of the Cu_5FeS_4 LSPR.**

Cu_5FeS_4 nanocrystals either in TCE solution (left) or dropcast (right) are compared utilizing the frequency-independent Drude modelling MATLAB code as performed previously by Milliron and coworkers.[3]

Figure S5. VT-MCD at 10 T.

VT-MCD is performed on Cu_5FeS_4 PSNCs in the NIR regime. An overall change in the signal in the MCD is observed, however there does not appear to be obvious C term behavior, rather only a slight temperature dependence on the overall signal is observable.

Figure S6. Zeeman Energy Fitting with associated effective mass.
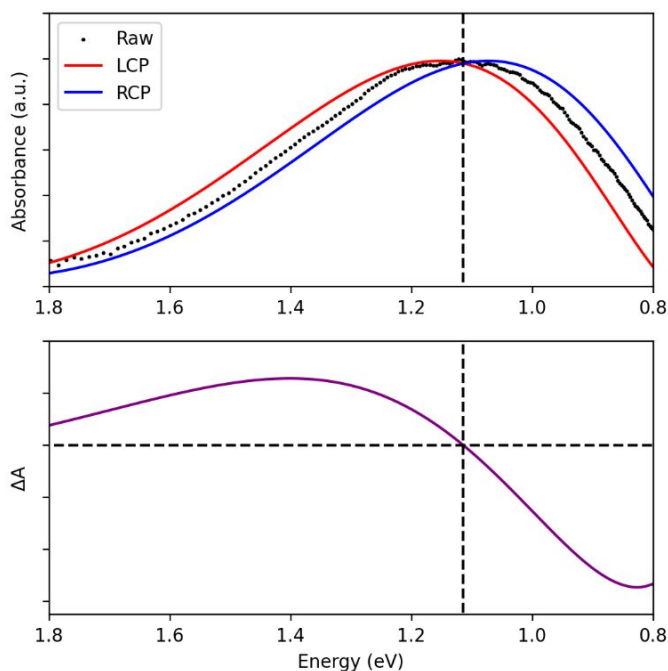

Description of m^* Acquisition from VH-MCD.

The linear absorption data for Cu_5FeS_4 was fit according to a combined version of Eqn. 6 and 7,

where m^* can be directly solved utilizing $m^* = \frac{qBc}{2\pi E_Z m_e}$ after obtaining an experimental E_Z term.

To obtain E_Z through an MCD spectrum, it is required to simulate separate LCP and RCP spectra

shifted by some constant energy, assuming the rigid-shift approximation (top) utilizing a known

experimental absorption spectrum. Once found, a custom least squares fitting program through

the Scipy.optimize.curve_fit() python package was used in order to optimize the Zeeman energy

difference separating the LCP and RCP spectra until the least squares fit was achieved, resulting

in a simulated MCD spectrum (bottom). The source code can be found at

https://github.com/strouselabgithub/strouselab.

Figure S7. Effective Mass Approximation Utilizing Data from Kumar et al.
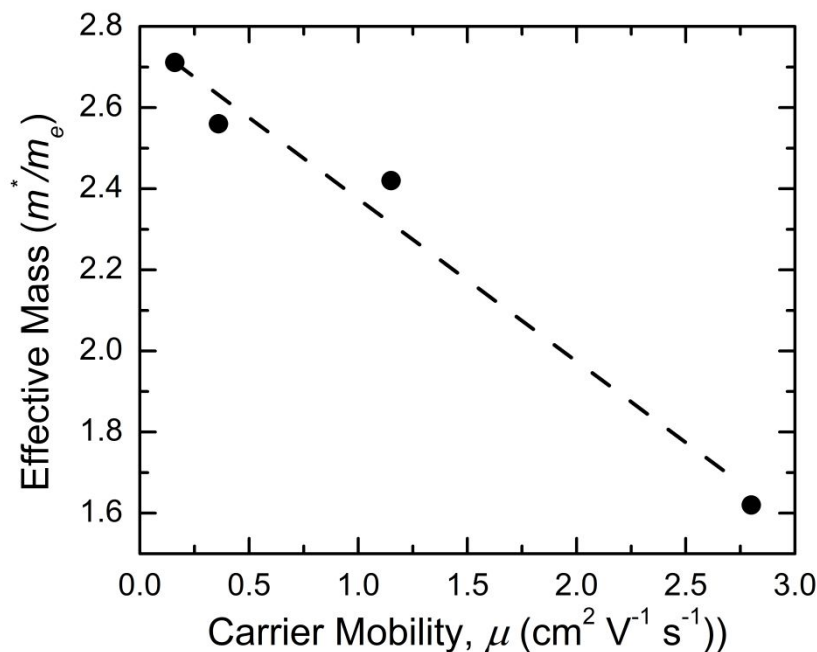
Utilizing the first principal relationship between the carrier effective mass, m^*, and the carrier mobility, μ, $m^* = \frac{\bar{\tau}q}{\mu}$, where $\bar{\tau}$ is the carrier scattering constant, and q is the electronic charge.

Taking tabulated data from Kumar et al. in experimental doping of Se into Cu_5FeS_4,[4] Assuming this linear relationship, the m^* can be approximated to first order, giving a result of 2.71 m^*/m_e, remarkably similar to the 2.73 m^*/m_e value obtained through experimental MCD at 2 T.

References.

(1) Kays, J. C.; Conti, C. R.; Margaronis, A.; Kuszynski, J. E.; Strouse, G. F.; Dennis, A. M. Controlled Synthesis and Exploration of CuxFeS4 Bornite Nanocrystals. *Chem. Mater.* **2021**, *33* (18), 7408–7416.
(2) Hartstein, K. H. Stabilizing Degenerate Dopants in Colloidal Semiconductor Nanocrystals. Ph.D., University of Washington, Ann Arbor, 2018.
(3) Mendelsberg, R. J.; Garcia, G.; Milliron, D. J. Extracting Reliable Electronic Properties from Transmission Spectra of Indium Tin Oxide Thin Films and Nanocrystal Films by Careful Application of the Drude Theory. *Journal of Applied Physics* **2012**, *111* (6), 063515.
(4) V. Pavan Kumar; Tristan Barbier; Pierric Lemoine; Bernard Raveau; Vivian Nassif; Emmanuel Guilmeau. The Crucial Role of Selenium for Sulphur Substitution in the Structural Transitions and Thermoelectric Properties of Cu5FeS4 Bornite. *Dalton Transactions* **2017**, *46* (7), 2174–2183.